LA-UR -86-3228 CONF-860701--72

Los Alamos National Laboratory is operated by the University of California for the United States Department of Energy under contract W-7405-ENG-36

LA-UR--86-3228

DE87 000155

TITLE: SEARCH FOR RARE MUON AND PION DECAY MODES WITH THE CRYSTAL BOX DETECTOR

AUTHOR(S): C. M. Hoffman, R. D. Bolton, J. D. Bowman, M. D. Cooper J. S. Frank, A. L. Hallin, P. Heusi, G. E. Hogan, F. G. Mariam, H. S. Matis, R. E. Mischke, D. E. Nagle, L. E. Piilonen, V. D. Sandberg, G. H. Sanders, U. Sennhauser, R. Werbeck, R. A. Williams, S. L. Wilson, R. Hofstadter, E. B. Hughes, M. W. Ritter, D. Grosnick, S. C. Wright, V. L. Highland, and J. McDonough

SUBMITTED TO: The Proceedings of the XXII International Conference on High Energy Physics, Berkeley, CA 7-16-23/86

Los Alamos Los Alamos National Laboratory Los Alamos, New Mexico 87545

FORM NO 836 R4
ST NO 2629 5/81

MASTER

DISTRIBUTION OF THIS DOCUMENT IS UNLIMITED

SEARCH FOR RARE MUON AND PION DECAY MODES WITH THE CRYSTAL BOX DETECTOR

C.M.Hoffman, R.D.Bolton, J.D.Bowman, M.D.Cooper, J.S.Frank, A.L.Hallin,[a] P.Heusi,[b] G.E.Hogan, F.G.Mariam, H.S.Matis,[c] R.E.Mischke, D.E.Nagle, L.E.Piilonen, V.D.Sandberg, G.H.Sanders, U.Sennhauser,[d] R.Werbeck, and R.A.Williams
Los Alamos National Laboratory, Los Alamos, New Mexico 87545

S.L.Wilson,[e] R Hofstadter, E.B.Hughes, and M.W.Ritter[f]
Stanford University, Stanford, California 94305

D.Grosnick and S.C.Wright
University of Chicago, Chicago, Illinois 60637

V.L.Highland and J.McDonough
Temple University, Philadelphia, Pennsylvania 19122

ABSTRACT

New experimental upper limits for the branching ratios of the lepton-family-number nonconserving decays $\mu^+ \to e^+\gamma$ and $\mu^+ \to e^+\gamma\gamma$ are presented. A new determination of γ, the ratio of pion axial-vector to vector form factors, from radiative pion decay is also reported. These results are from data taken with the Crystal Box detector at LAMPF.

RARE MUON DECAYS

No process violating conservation of lepton family number, like $\mu^+ \to e^+\gamma$ or $\mu \to e^+\gamma\gamma$, has ever been seen. Such processes are forbidden in the minimal standard model[1] of electroweak interactions. However, it is widely believed that the standard model is incomplete. Many extensions to the model have been proposed such as including massive neutrinos, an expanded Higgs sector, or supersymmetry. In general, lepton family number need not be conserved in these extensions. The existing experimental upper limits for the rates of these processes impose model-dependent constraints on the theoretical parameters, like mixing angles or gauge-boson masses, that describe these processes.[2]

Prior to this experiment, the best experimental upper limits of the branching ratios (90% C.L.) for $\mu^+ \to e^+\gamma$ and $\mu^+ \to e^+\gamma\gamma$ were[3,4] $B_{e\gamma} \lesssim 1.7 \times 10^{-10}$ and $B_{e\gamma\gamma} \lesssim 8.4 \times 10^{-9}$, respectively. We report here improved limits for $B_{e\gamma}$ and $B_{e\gamma\gamma}$ from data taken with the Crystal Box detector in the stopped muon channel at LAMPF.

The Crystal Box detector,[5] shown in Fig. 1, consists of 396 NaI(Tℓ) crystals, 36 plastic scintillation hodoscope counters, and a cylindrical 8-plane stereo drift chamber[6] surrounding a thin planar polystyrene target where positive muons decay at rest. Positron trajectories are measured in the drift chamber. The position resolution of the intersection of the positron trajectory and the target is 2mm. Electromagnetic showers from positrons and photons are detected in the NaI(Tℓ). The photon conversion point is determined to 4.7 cm by examining the energy sharing among the NaI(Tℓ) crystals. The NaI(Tℓ) energy resolution is ~ 7%. The timing resolution of the NaI(Tℓ) (for photons) is 1.2 ns and of the scintillators (for positrons) is 0.29 ns. (All resolutions are FWHM.)

The data for $\mu^+ \to e^+\gamma$ and $\mu^+ \to e^+\gamma\gamma$ were collected concurrently. The muon stopping rate was ~500 kHz with a duty factor of ~7%. Data written on magnetic tape for each candidate rare-decay event included timing and energy information from all hodoscope counters and from those NaI(Tℓ) crystals with at least 0.1 MeV deposited energy, and timing information from the drift-chamber cells that were hit.

The apparatus acceptances for the rare decay modes were determined with a Monte Carlo simulation, based on the shower code EGS3,[7] that accurately reproduced the response of the detector to photons, positrons, and electrons.

The $\mu^+ \to e^+\gamma$ data analysis is presented first. The signature for a $\mu^+ \to e^+\gamma$ decay at rest is a positron and a

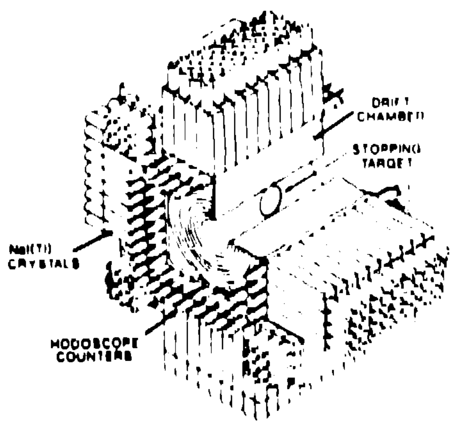

Fig. 1. The Crystal Box.

photon back-to-back, in time coincidence, with $E_e = E_\gamma = 52.8$ MeV. The hardware trigger for $\mu^+ \to e^+\gamma$ required a coincidence within ±5 ns of a "positron quadrant" and an opposite "photon quadrant", with at least 30 MeV deposited in the NaI(Tℓ) of each of these quadrants. A positron quadrant had a hodoscope counter signal and one or more NaI(Tℓ) discriminator signals. A photon quadrant had no hodoscope counter signal and at least one NaI(Tℓ) discriminator signal. The trigger selected ~ 10^7 candidates from ~ 10^{12} muon decays. These events can be due to $\mu^+ \to e^+\gamma$, $\mu^+ \to e^+\nu\bar{\nu}\gamma$ (inner bremsstrahlung) and random coincidences.

The offline data reduction retained for subsequent analysis all $\mu^+ \to e\gamma$ events and an appreciable number of inner bremsstrahlung events and random coincidences. A total of 17 073 events satisfied $|\Delta t_{e\gamma}| < 5$ ns, $\theta_{e\gamma} \geq 160°$, $E_e \geq 44$ MeV, and $E_\gamma \geq 40$ MeV. Figure 2a shows $\Delta t_{e\gamma}$, the photon-positron relative timing, for a subset of these events. The broad distribution is due to random coincidences, while the prompt peak is due to inner bremsstrahlung and possibly $\mu^+ \to e^+\gamma$.

The $\mu^+ \to e^+\gamma$ content was found by maximizing the likelihood

$$L(n_{e\gamma}, n_I) = \prod_{i=1}^{N} \left[\frac{n_{e\gamma}}{N} P(\vec{x}_i) + \frac{n_I}{N} Q(\vec{x}_i) + \frac{n_R}{N} R(\vec{x}_i) \right]$$

with respect to the parameters $n_{e\gamma}$, n_I, and $n_R = N - n_{e\gamma} - n_I$ that estimated the number of $\mu^+ \to e^+\gamma$, inner bremsstrahlung, and random events, respectively, in the total sample of N events. The vector $\vec{x}$ has components $\theta_{e\gamma}$, $\Delta t_{e\gamma}$, E_e, and E_γ. P, Q, and R are the probability distributions for $\mu^+ \to e^+\gamma$, inner bremsstrahlung and random events, respectively. The distributions for P and Q were determined from the Monte Carlo program, while R came from out-of-time events.

Figure 3 shows the normalized likelihood function. It peaks at $n_{e\gamma} = 0$ and $n_I = 3470 \pm 80 \pm 300$ events. The latter agrees well with the 3960 ± 90 ± 200 inner bremsstrahlung events expected in the data. The likelihood function distribution implies $n_{e\gamma} < 11$ events (90% C.L.). Using the number of muons stopped, 1.35×10^{12}, during the live time of the experiment, the apparatus acceptance for $\mu^+ \to e^+\gamma$, 0.305, and the detection efficiency, 0.545, we obtain $B_{e\gamma} < 4.9 \times 10^{-11}$. Figure 2a-d shows the agreement between the data (histogrammed) and the best mix of $\mu^+ \to e^+\nu\bar{\nu}\gamma$ and randoms (smooth) as determined by the likelihood analysis.

The analysis of the $\mu^+ \to e^+\gamma\gamma$ data is presented next. The signature for a $\mu^+ \to e^+\gamma\gamma$ decay at rest is a positron and two photons in time coincidence emerging with zero net momentum and $E_{tot} = E_e + E_{\gamma 1} + E_{\gamma 2} = 105.6$ MeV. The three particles could strike two quadrants of the Crystal Box and fire the eγ trigger discussed above, or could strike three quadrants and fire the eγγ trigger. The $\mu^+ \to e^+\gamma\gamma$ trigger required a time coincidence within ±5 ns of a positron quadrant and two photon quadrants, with at least 70 MeV deposited in the NaI(Tℓ) calorimeter.

The eγγ trigger recorded ~ 10^6 candidates. In addition, ~ 10^5 candidates were found in the eγ-triggered events, where the positron and one photon occupied the same quadrant. Figure 4 shows the relative timing distribution for some of these events, the majority being backgrounds from triple random coincidences or two-particle prompt events in random coincidence with a third particle (e.g., $\mu^+ \to e^+\nu\bar{\nu}\gamma + \gamma$).

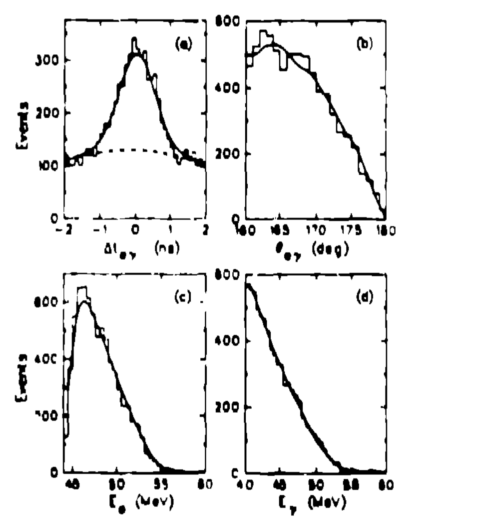

Fig. 2. Histograms of eγ candidates.

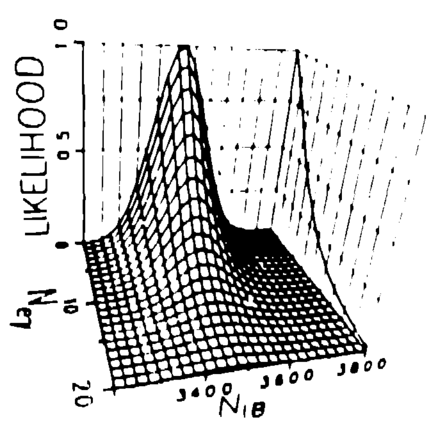

Fig. 3. $\mu \to e\gamma$ likelihood function.

The offline analysis removed most of the random coincidences while retaining all of the $\mu^+ \to e^+\gamma\gamma$ events, assuming the most general local interaction for the $\mu^+ \to e^+\gamma\gamma$ matrix element.[8] Events with one particle showering and appearing as two hits in the trigger were removed by energy and opening-angle cuts. Figure 5 shows the distribution of events vs $\tau = 2t_e - t_{\gamma 1} - t_{\gamma 2}$ for the 272 events passing these cuts. No appreciable coincidence signal can be seen in this plot. A final cut requiring each photon energy to be greater than 20 MeV leaves nine candidate events. These nine events are shaded in Fig. 5.

The number of $\mu^+ \to e^+\gamma\gamma$ events in the sample of nine events was estimated by maximizing the likelihood

$$L(n_{e\gamma\gamma}) = \prod_{i=1}^{N} \left[\frac{n_{e\gamma\gamma}}{N} P(\vec{x}_i) + \frac{n_R}{N} R(\vec{x}_i) \right]$$

with respect to the parameters $n_{e\gamma\gamma}$ and $n_R = N - n_{e\gamma\gamma}$ that estimated the number of $\mu^+ \to e^+\gamma\gamma$ and background events in the sample of N events. P and R are the probability distributions for $\mu^+ \to e^+\gamma\gamma$ and background, respectively. The components of $\vec{x}$ are E_{tot}, τ, $p_\perp = |\vec{p}_a + \vec{p}_b + \vec{p}_c \times \hat{p}_{ab}|$ and $\cos\alpha = \hat{p}_c \cdot \hat{p}_{ab}$, where $\vec{p}_a$ and $\vec{p}_b$ are the momenta most nearly perpendicular to each other, $\hat{p}_{ab}$ is the unit vector normal to the p_a-p_b plane, and $\vec{p}_c$ was the third particle's momentum.

The likelihood function distribution in Fig. 6 implies $n_{e\gamma\gamma} < 2.9$ (90% C.L.). Using the number of muons stopped, 8.2×10^{11}, during the live time of the experiment, the apparatus acceptance for $\mu^+ \to e^+\gamma\gamma$, 0.064, and the detector efficiency, 0.524, we obtain $B_{e\gamma\gamma} < 7.2 \times 10^{-11}$ (90% C.L.).

RADIATIVE PION DECAY

The low-energy behavior of QCD, the strong-interaction component of the standard model, is extremely difficult to determine. Nevertheless, there are serious attempts to calculate low-energy parameters such as the ratio $\gamma = F_A/F_V$ of the pion weak axial-vector to vector form factors.[9] This ratio can be measured in the radiative decay of the pion, $\pi^+ \to e^+\nu_e\gamma$, where the decay rate is determined by the coherent admixture of an amplitude sensitive to the strong interaction (γ dependent[10]) and an amplitude that accounts for QED corrections to the decay $\pi^+ \to e^+\nu_e$.

The results of two previous measurements[11,12] are ambiguous because the experiments detected photons and positrons in a region of phase space where the term in the decay rate proportional to $(1+\gamma)^2$ dominates. The weighted averages of γ are $\gamma = 0.41 \pm 0.06$ or $\gamma = -2.36 \pm 0.06$. We report here data that resolves the ambiguity in the measurement of γ.

Pions passed through a CH_2 degrader and a segmented scintillation beam counter, then stopped and decayed in a planar CH_2 target in the Crystal Box. The trigger required a coincidence within ±5 ns of a positron quadrant and an opposite photon quadrant; these signals had to appear within 50 ns of a signal from the beam counters. The trigger recorded ~ 10^7 candidates from 4×10^{10} pion decays. Events from $\mu^+ \to e^+\nu\bar{\nu}\gamma$ were eliminated by requiring $E_e + E_\gamma + |\vec{p}_e + \vec{p}_\gamma| > 115$ MeV. Events with $E_\gamma \geq 25$ MeV, $E_e \geq 15$ MeV, either $E_\gamma \geq 50$ MeV or $E_e \geq 53$ MeV, and $105° \leq \theta_{e\gamma} < 180°$, were retained for subsequent analysis. These events are from $\pi^+ \to e^+\nu_e\gamma$ or are random coincidences.

The distribution of events in phase space was used to resolve the ambiguity in γ. We maximized the likelihood

$$L(n_{e\nu\gamma}, \gamma) = \prod_{i=1}^{N} \left[\frac{n_{e\nu\gamma}}{N} P_\gamma(\vec{x}_i) + \frac{n_R}{N} R(\vec{x}_i) \right]$$

by varying the ratio γ and the parameters $n_{e\nu\gamma}$ and $n_R = N - n_{e\nu\gamma}$ that estimated of the number of $\pi^+ \to e^+\nu_e\gamma$ and random events in the sample of N events. P_γ and R are the probability distributions for $\pi^+ \to e^+\nu_e\gamma$ (for a particular value of γ) and randoms, respectively. The coordinates of $\vec{x}$ are $\theta_{e\gamma}$, $\Delta t_{e\gamma}$, E_e, and E_γ.

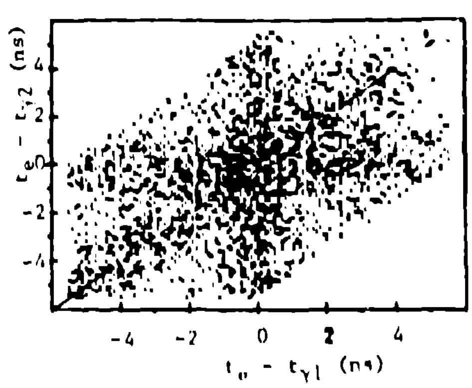

Fig. 4. Scatter plot of $e\gamma\gamma$ candidates.

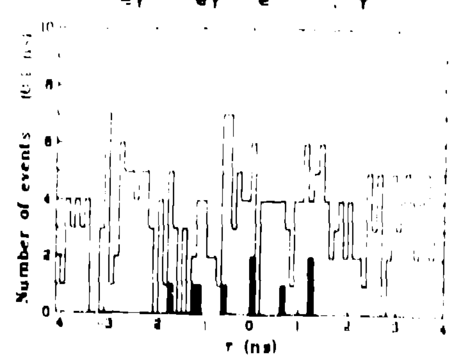

Fig. 5. τ distribution.

Figure 7 shows the normalized likelihood as a function of γ. The positive value for γ is favored over the negative value by a likelihood ratio of 2175 to 1.

The ratio of the number of prompt events with either $E_\gamma \geq 43$ MeV or $E_e \geq 53$ MeV to the number of pion stops (corrected for $\pi^+ \to e^+\nu_e\gamma$ detection efficiency) gave the measured branching ratio for $\pi^+ \to e^+\nu_e\gamma$ in this region. Comparing this measurement to the branching ratio calculated as a function of γ, we find $\gamma = 0.22 \pm 0.15$ or $\gamma = -2.13 \pm 0.15$, in agreement with the previous measurements.

Thus we obtain the unique solution $\gamma = 0.25 \pm 0.12$. The new world average is $\gamma = 0.39 \pm 0.06$.

SUMMARY

Using data from μ^+ decays in the Crystal Box detector, we have obtained improved upper limits on the branching ratios of the lepton-family-number nonconserving decays $\mu^+ \to e^+\gamma$ and $\mu^+ \to e^+\gamma\gamma$ of $B_{e\gamma} < 4.9 \times 10^{-11}$ and $B_{e\gamma\gamma} < 7.2 \times 10^{-11}$, respectively. Using data from π^+ decays, we have resolved the ambiguity in the measurement of γ, the ratio of pion axial-vector to vector form factors, in favor of the positive value, with a new world average of $\gamma = 0.39 \pm 0.06$.

We acknowledge the extraordinary assistance from the many people at each of our institutions and from the operations staff at LAMPF. This work was supported in part by the U.S. Department of Energy and the National Science Foundation.

REFERENCES

a. Now at Physics Dept., Princeton University, Princeton, NJ 08544
b. Now at ELEKTROWATT Ing. AG., Zurich, Switzerland
c. Now at Lawrence Berkeley Laboratory, Berkeley, CA 94720
d. Now at SIN, CH-5234 Villigen, Switzerland
e. Now at Los Alamos National Laboratory, Los Alamos, NM 87545
f. Now at Lockheed Missiles and Space Company, Palo Alto, CA 94304

1. S.L. Glashow, Nucl. Phys. 22, 579 (1961); S. Weinberg, Phys. Rev. Lett. 19, 1264 (1967); A. Salam, in Elementary Particle Theory: Relativistic Groups and Analyticity (Nobel Symposium No. 8), ed. N. Svartholm (Almqvist and Wiksells, Stockholm, 1968), p. 367.
2. C.M. Hoffman, in Fundamental Interactions in Low-Energy Systems, ed. P. Dalpiaz et al., (Plenum Press, New York, 1985), p. 138; P. Herczeg and T. Oka, Phys. Rev. D29, 475 (1984); D.E. Nagle, Comments on Nuclear and Particle Physics XI, 277 (1983).
3. W.W. Kinnison et al., Phys. Rev. D25, 2846 (1982).
4. G. Azuelos et al., Phys. Rev. Lett. 51, 164 (1983).
5. R.D. Bolton et al., Phys. Rev. Lett. 56, 2461 (1986) and references therein.
6. R.D. Bolton et al., Nucl. Instr. and Methods 241, 52 (1985).
7. R.L. Ford and W.R. Nelson, Stanford Linear Accelerator Center No. SLAC-210, 1978 (unpublished).
8. J.D. Bowman et al., Phys. Rev. Lett. 41, 442 (1978).
9. B.R. Holstein, Phys. Rev. D33, 3316 (1986).
10. D.A. Bryman et al., Phys. Rep. 88, 151 (1982).
11. A. Stetz et al., Nucl. Phys. B4, 189 (1978).
12. A. Bay et al., Proceedings of Tenth International Conference on Particles and Nuclei, Heidelberg (1984).

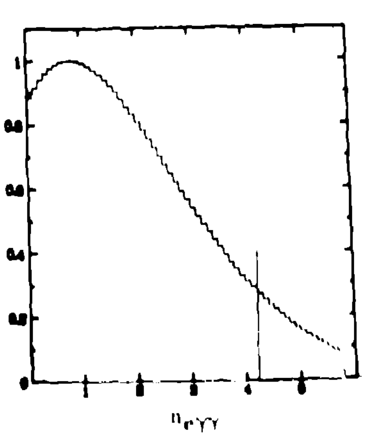

Fig. 6 The likelihood function.

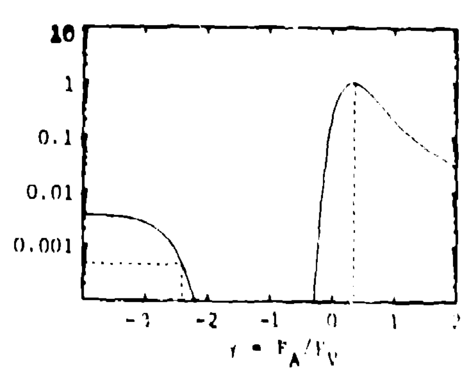

Fig. 7. $\pi \to e\nu\gamma$ likelihood.